Article

JFPE

Journal of Fire Protection Engineering
22(3) 183–196

DOI: 10.1177/1042391512447045
jfe.sagepub.com

SAGE

Elevated temperature deflection behavior of concrete members reinforced with FRP bars

MA Faruqi
Department of Civil and Architectural Engineering, Texas A&M University-Kingsville, Kingsville, TX, USA

S Roy
Department of Civil and Architectural Engineering, Texas A&M University-Kingsville, Kingsville, TX, USA

A Salem
Department of Mechanical Engineering, Rochester Institute of Technology, Dubai

Abstract
In recent years there has been an increased interest in the use of fiber reinforced polymer (FRP) materials in concrete members. However, the behavior of such members in fire is still relatively unknown. Since this is the main reason limiting the widespread use of FRP in buildings, the use of FRP in fire vulnerable structures needs additional study. In this article, a model is developed that incorporates the temperature dependent progressive changes of Elastic-modulus of FRP in predicting the deflection behavior of FRP reinforced concrete structures within the range of practical elevated temperatures. Predictions from the model correlate well with experimental results from the literature. The new approach provides an additional tool to evaluate the deflection of FRP reinforced concrete structures in fire.

Keywords
Concrete, fiber-reinforced polymer reinforcement, fire, glass-transition, practical elevated temperatures, deflection

Corresponding author:
MA Faruqi, Department of Civil and Architectural Engineering, Texas A&M University-Kingsville, MSC 194, Kingsville, TX 78363, USA
Email: m-faruqi@tamuk.edu

Introduction

Deterioration of infrastructure resulting from corrosion of steel reinforcement in concrete has led to the use of fiber-reinforced polymer (FRP) composites as an alternative. High strength to weight ratio and corrosion resistance of FRP rebars provides a significant advantage over steel [1]. FRP reinforcement is used in bridges, multi-storied buildings, industrial structures and parking garages to name a few. In order to design FRP reinforced concrete structures subject to elevated temperatures, it is important to understand some of the thermo-mechanical properties (stiffness, strength) of the FRP reinforcement within the range of practical temperatures.

The design behavior of FRP reinforced (rebar) concrete structures is well known at ambient temperatures [2–4]. However, its behavior at elevated temperatures is quite complex and as a result the codes do not specify any fire guidelines. The American Concrete Institute (ACI) code merely recommends that FRP reinforced concrete structures must meet all building and fire code requirements that apply to a typical reinforced concrete structure [4]. The British Standard BS 476 [5] and BS 9999 [6] consider deflection and structural fire resistance as factors to determine beam failure. These codes respectively provide a maximum allowable deflection of L/20 and a minimum of 90 min of fire resistance.

At higher temperatures, the concrete gets de-moisturized rapidly and produces cracks. This causes the FRP rebar to burn and eventually de-bond [7]. Thermo-mechanical behavior of FRP rebar depends on the polymer resin [7]. The polymer resin will soften and the FRP bar reaches its glass transition temperature rapidly. Elastic modulus (E-modulus) of the polymer decreases significantly when the temperature reaches and exceeds glass transition temperature [7]. The glass transition region is the most significant practical region of FRP for design purposes. This is because the system undergoes significant plastic deformations beyond this region resulting in structural collapse [8–10]. At this transition temperature, the resin is no longer able to transfer stresses from concrete to fibers. This leads to increased crack widths and deflections. The deflection is directly related to the progressive changes in the E-modulus of FRP composites under elevated temperatures. Unfortunately, this topic has received very little attention from the research community and therefore lacks design specifications. The current study examines the effect of fire on the deflection behavior of FRP reinforced concrete structures and accounts for the temperature-dependent progressive changes in the E-modulus of FRP within the range of practical elevated temperatures.

Materials and experimental setup

Experimental data from fire tests of concrete beams reinforced with FRP were obtained by Abbasi and Hogg [11]. A brief description of these tests is provided here for the convenience of the reader. Two FRP reinforced concrete beams were cast for testing at elevated temperatures. Cross sections of the beams were 350×400 mm^2 and the total length of the specimens were 4250 mm. Glass fiber reinforced polymer (GFRP) #4 rebar was used. The first beam and second beams used special GFRP rebar containing a vinyl ester and polyurethane resin matrix respectively, with

a 75 mm concrete cover. This ensured integrity at elevated temperatures. The E-modulus of the rebar was 41 GPa. The GFRP surface was wrapped with a helical fiber having a pitch of about 25.4 mm to produce traction on the bar surface. To avoid shear failure traditional #3 U shaped stirrups were used. There were seven bars at the bottom of the beam and two at the top. All beams were designed to fail through the mechanism of concrete crushing as recommended by ACI 440 [2]. This was accomplished with a reinforcement ratio greater than the balanced ratio. A ρ_f/ρ_b ratio of 1.98 was used. A control beam with dimensions and reinforcement similar to the first beam was also cast and tested at room temperature. Type I cement was used in concrete mix, which had a water to cement ratio of 0.38. To increase the strength of the concrete, a water reducing admixture composition that was 1% of the cement was used. The average size of coarse aggregate was 20 mm and that of fine aggregate, 10 mm. Further details of the experimental setup and testing can be found in [11].

Mechanical properties of FRP in a fire

The mechanical properties of FRP composites vary significantly when subjected to elevated temperatures. This is due to their molecular bonds [12]. In the lower temperature range, the bonds are intact and therefore correspond to a horizontal segment of E-modulus. This is known as the glassy state. However, as the temperature increases, more bonds are weakened and a new state is reached [12]. This new state is referred to as the leathery state. The region between glassy and leathery state is known as the glass transition zone. As the temperature rises, further break down of bond leads to the rubbery state. The region between leathery and rubbery states is known as the leathery zone [12]. When temperatures are further elevated, a decomposed state is reached via a rubbery zone. The most significant practical region of FRP for design purposes in fire is the glass transition temperature. This is because the system undergoes significant plastic deformations at and beyond this region [7]. Figure 1 shows the approximate states and polymer transitions at elevated temperatures [13]. Figure 2 shows a generalized glass transition zone.

Proposed approach

Formulation of E-modulus

The E-modulus of FRP can be calculated as follows: A unidirectional composite can be modeled by assuming fibers to be continuous and parallel throughout the composite. Also, assume a perfect bond exists between fibers and the matrix. This model is shown in Figure 3.

The strains experienced by fiber, matrix, and composite are assumed to be equal. Therefore, the load carried by the total system is shared between fibers and matrix. This means

$$P_c = P_{\text{frp}} = P_f + P_m \tag{1}$$

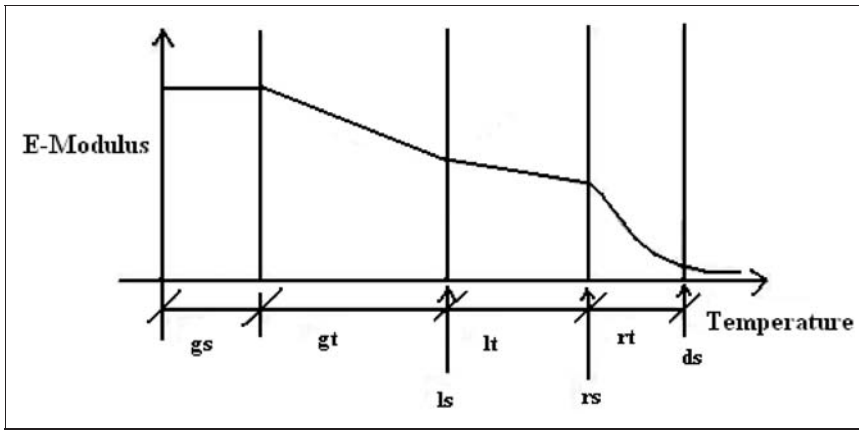

Figure 1. Approximate states and transitions of a polymer at elevated temperatures.
gs: glassy state $\leq 250^{\circ}C$; gt: glass transition zone (approximate), $230^{\circ}C \leq gt \leq 435^{\circ}C$; ls: leathery state and glass transition temperature ($\approx 435^{\circ}C$); lt: leathery zone; rs: rubbery state; rt: rubbery zone, $600^{\circ}C \leq rt \leq 900^{\circ}C$; ds: decomposed state $> 900^{\circ}C$.

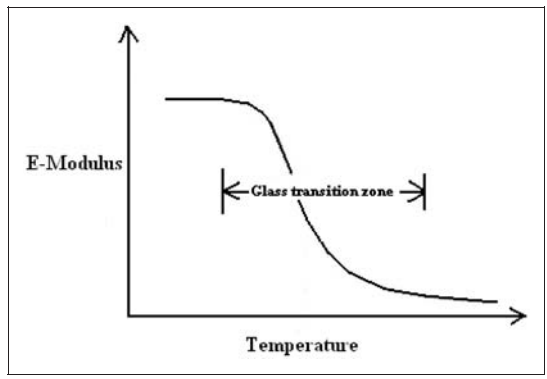

Figure 2. Generalized glass transition zone.

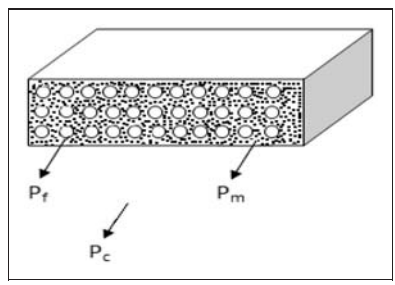

Figure 3. Model of unidirectional composite.

Considering the fibers to be glass, the equation in terms of stresses becomes

$$\sigma_{\text{frp}} = \sigma_g(A_g/A_{\text{frp}}) + \sigma_m(A_m/A_{\text{frp}}) \tag{2}$$

Equating area fractions to volume fractions, differentiating with respect to strain, substituting E-moduli, and simplifying yields

$$\mathrm{d}\sigma_{\text{frp}}/\mathrm{d}\varepsilon = (\mathrm{d}\sigma_g/\mathrm{d}\varepsilon)V_g + (\mathrm{d}\sigma_m/\mathrm{d}\varepsilon)V_m \tag{3}$$

$$E_{\text{frp}} = E_g V_g + E_m V_m \tag{4}$$

Therefore

$$E_{\text{frp}}/E_m = (E_g/E_m - 1)V_g + 1 \tag{5}$$

Noting that $E_m\ V_m$ is a standard term for matrix, that $E_{lt}\ V_{lt}$ is the state of matrix in the leathery zone, and that temperature at a particular section is considered constant, then substituting $E_{lt}\ V_{lt}$ for $E_m\ V_m$ in equation (4) yields:

$$E_{\text{frp}} = E_g V_g + E_{lt} V_{lt} \tag{6}$$

Development of deflection model at elevated temperatures

At higher temperatures, the concrete gets de-moisturized rapidly, dries, shrinks, and produces cracks. This concrete behavior causes the FRP rebar in the beam to be compromised. The resultant deflection depends on the shrinkage curvature and the support conditions of the FRP reinforced system exposed to elevated temperatures. Figure 4 shows the basic temperature-based shrinkage causing deflection.

This type of deflection can be expressed as:

Deflection = constant × shrinkage curvature due to elevated temperature × L.

$$\Delta_{\text{et}} = K_S \Phi_{\text{et}} L \tag{7}$$

$$\Phi_{\text{et}} = 2T_h e/(E_{\text{conc}} I_{\text{eff}}) \tag{8}$$

Where e is the distance from the tension reinforcement to the neutral axis

$$T_h = \left(A_{\text{frp}} + A'_{\text{frp}}\right)\varepsilon_h E_{\text{frp}} \tag{9}$$

Substitution of T_h and Φ_{et} into equation (7), and simplifying yields

$$\Delta_{\text{et}} = \left\{2K_S e L/I_{\text{eff}}\right\}\left[\left\{\left(A_{\text{frp}} + A'_{\text{frp}}\right)\varepsilon_h E_{\text{frp}}\right\}/E_{\text{conc}}\right] \tag{10}$$

One of the important factors in determining the properties of a composite is the relative proportion of volume at various states and temperatures. Consider a unit volume of FRP material at a particular temperature. The volume of the material [13] at a practical state can be obtained as

$$V_g = (1 - \alpha_g) \text{ and } V_{lt} = (1 - \alpha_g)(1 - \alpha_d) \tag{11}$$

Substituting the volumes at glass and leathery transition states into equation (6) yields

$$E_{\text{frp}} = E_g(1 - \alpha_g) + E_{lt}(1 - \alpha_g)(1 - \alpha_d) \tag{12}$$

Equations provided in Saafi [14] are not accurate for the special GFRP rebar with a glass transition zone of 230–435°C. Therefore, the equations in [14] are modified to address this new situation, as follows. $E_g \approx M_r E_{frp,\,20^\circ\text{C}}$ where $E_{\text{frp},\,20^\circ\text{C}}$ is approximately $4.10 \times 10^4 \text{N/mm}^2$ and

$$M_r \approx 1;\ 0 \le T \le 100 \tag{13}$$

$$M_r \approx 1 - 0.00188T;\ 100 \le T \le 300 \tag{14}$$

$$M_r \approx 1 - 0.0023T;\ 300 \le T \le 435 \tag{15}$$

$$M_r \approx 0;\ T > 435 \tag{16}$$

Substituting equation (12) into equation (10) then provides

$$\Delta_{\text{et}} = \left[\left\{2K_S e L\left(A_{\text{frp}} + A'_{\text{frp}}\right)\varepsilon_h\right\}/I_{\text{eff}}\right]\left[\left\{E_g(1 - \alpha_g) + E_{lt}(1 - \alpha_g)(1 - \alpha_d)\right\}/E_{\text{conc}}\right] \tag{17}$$

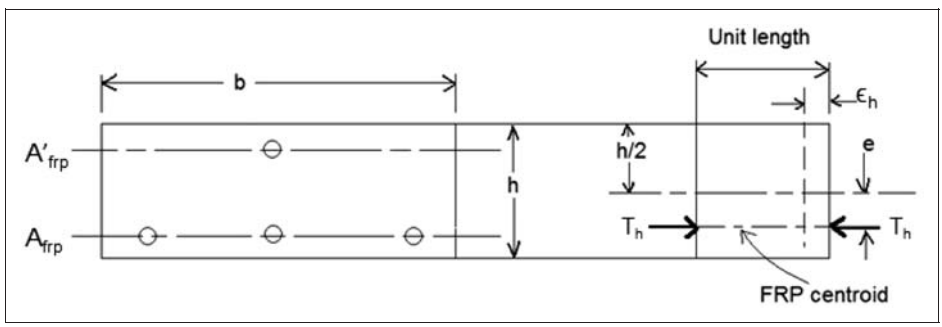

Figure 4. Temperature-based deflection in a FRP reinforced concrete beam.

Considering that $E_g/E_{\text{conc}} = n_g$; $E_{lt}/E_{\text{conc}} = n_{lt}$ and $\left[\left\{2K_S eL\left(A_{\text{frp}} + A'_{\text{frp}}\right)\right\}/I_{\text{eff}}\right] = \psi$, gives the result:

$$\Delta_{\text{et}} = \psi\varepsilon_h\left[n_g\left(1-\alpha_g\right) + n_{lt}\left(1-\alpha_g-\alpha_d-\alpha_g\alpha_d\right)\right] \tag{18}$$

Since $\alpha_g\ \alpha_d \approx 0$ as the product is very small, the expression becomes

$$\Delta_{\text{et}} = \psi\varepsilon_h\left[n_g\left(1-\alpha_g\right) + n_{lt}\left(1-\alpha_g-\alpha_d\right)\right] \tag{19}$$

Where $\varepsilon_h \approx \alpha'_g T_{\text{frp}}$. For practical purposes, only temperatures up to 435°C (glass transition temperature) are considered.

Therefore, E_{lt} can be approximated as zero. This implies that $n_{lt}(1–\alpha_g–\alpha_d) = 0$

Substituting ε_h and $\psi n_g \alpha'_g\left(1-\alpha_g\right) = \xi$ into equation (19) provides the deflection in the glass transition zone:

$$\Delta_{\text{et}} = \xi T_{\text{frp}} \tag{20}$$

Comparison of results

Figures 5 and 6 show a comparison of the model with experimental results from the literature [11] for beams 1 and 2, respectively. In Figure 5, the approximate glass transition zone ranges from 300°C to 435°C with approximate model values respectively ranging from 33.1 to 159.4 mm ($\approx L/28$) as compared to 33.9 and 178.1 mm. Similarly, for beam 2 the approximate model values respectively range from 31.1 to 150.62 mm as compared to 32.09 to 157.91 mm ($\approx L/29$) for the approximate glass

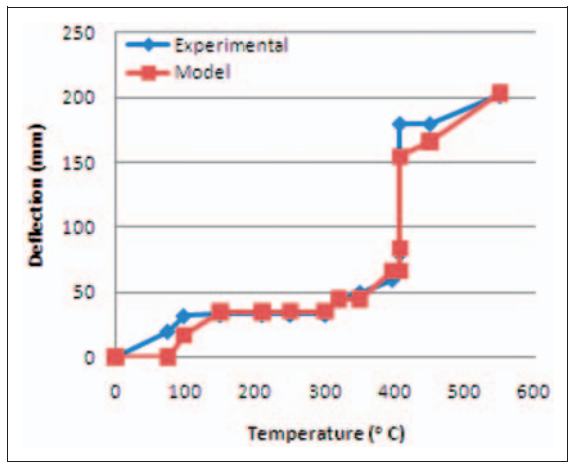

Figure 5. Comparison of results for Beam 1.

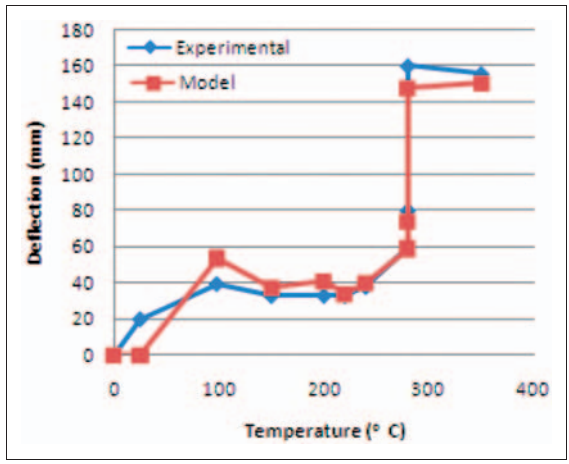

Figure 6. Comparison of results for Beam 2.

transitional temperature range of 230–335°C. The predicted deflections are lower than the safe limit specified by BS 476. Sudden deflections in beams 1 and 2 are respectively seen at approximate temperatures of 407°C and 280°C. This can be attributed to the fact that the polymeric material underwent a change from hard and brittle to viscous at approximate glass transition temperatures. At this temperature, the resin is no longer able to transfer stresses from concrete to fibers. Figure 7 shows a comparison of E-modulus with experimental results from the literature [10]. A similar trend of strength loss at glass transition temperatures is observed.

Application

FRPs are high performance materials and offer a wide range of applications. However, when used in building applications, they need to conform to fire resistance ratings stated in the building codes. There has been a limited effort to develop solutions for understanding required fire endurance of FRPs, as the current approaches to fire resistance through standard fire tests are expensive and time consuming. The provisions provided in the building codes for fire resistance evaluation are prescriptive and are not applicable to performance-based design that provides rational solutions under realistic scenarios. The preceding predictive modeling and evaluation of beams tests has led to a cost effective, efficient and practical performance-based method for fire safety design.

Parametric estimation is an important aspect of a practical fire-based design. The modulus of elasticity of FRP reinforcement is lower than that of steel. Therefore, FRP reinforced members typically display larger deflections than equivalent steel reinforced members at ambient temperatures. This means the support conditions need to be incorporated to reflect this, in particular, relatively large

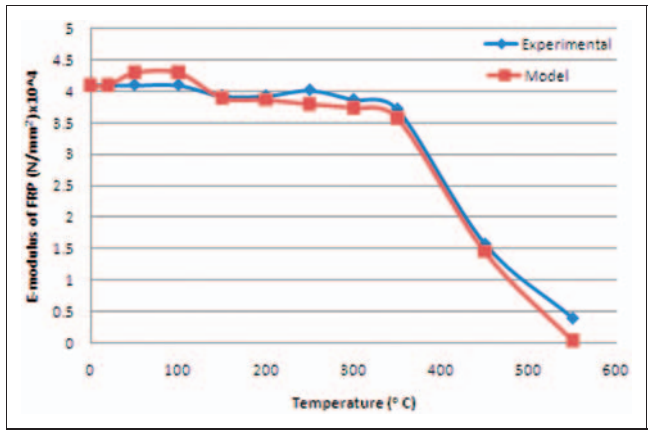

Figure 7. Comparison of E-modulus.

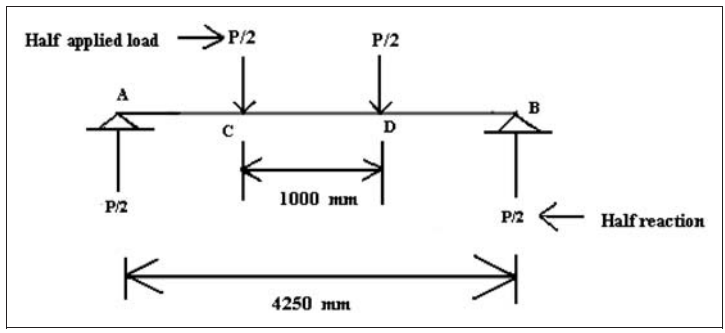

Figure 8. A simply supported beam subjected to a four-point loading.

deflections due to elevated temperatures. For practical applications and depending on the importance of the design, glass conversion factors can be estimated to be 1–4.5% of the unit glass volume up to glass transition temperature. Also, for practical applications and based on the latest conclusions of ACI 435R [15], a semi fixed support system can safely be assumed. An example together with explanations to calculate beam deflection is presented in the following discussion.

A rectangular, doubly FRP reinforced concrete beam using a four point loading system is shown in Figure 8. The two vertical loads are 1000 mm apart. The supported span is 4250 mm. End supports are semi-fixed. Other parameters are: $P = 440$ kN; beam cross-section is 350 mm × 400 mm; cover = 75 mm overall; $f'_c = 42$ N/mm^2; $A_{\text{frp}} = 1013.90$ mm^2; $A'_{\text{frp}} = 289.70$ mm^2; $e = 125$ mm; $K_s = 0.49$; $E_{\text{conc}} = 30.65$ kN/mm^2; $E_{\text{frp, 20°C}} = 4.15 \times 10^4$ N/mm^2; $E_{\text{frp, 435°C}} \approx 3.60 \times 10^4$ N/mm^2; $\alpha_g = 0.0465$; $\Delta_{\text{exp}} \approx 178.1$ mm; $T_{\text{frp}} \approx 435$°C, which is chosen as this is the approximate glass transition temperature.

The beam cross-section and the dimensions of the transformed area are shown in Figure 9.

In order to calculate the beam deflection at elevated temperature (Δ_{et}), the deflection constant (ψ) is needed. However, this constant is a function of effective moment of inertia (I_e) and other parameters. The I_e value depends on actual moment (M_a), cracked moment of inertia (I_{cr}), gross moment of inertia (I_g), and cracking moment (M_{cr}) of the beam. Calculations of M_a, I_{cr}, I_g, M_{cr}, I_e, ψ, and Δ_{et} are shown in the following paragraphs.

Maximum actual moment in the beam occurs at point C in Figure 8. This moment can be calculated as: $M_a = P/2$ * distance AC $\approx 220 \times (1.62) = 356$ kN-m.

Tensile cracks that develop in the beam will, in effect, cause the beam cross-section to be reduced. The cracked beam starts to lose strength as these cracks appear. For this reason, I_{cr} is important. The I_{cr} value can be calculated using the transformed area diagram shown in Figure 9. In this diagram, the FRP is transformed to an equivalent (i.e. same axial stiffness) area of concrete. The location of the neutral axis (x), shown in Figure 9 is a function of modular ratio (n) and tension reinforcement area (A_{frp}). The modular ratio for the transformed area $= E_{frp}/E_{conc} = 41.50/30.65 = 1.35$. The first moment of the compression area about the neutral axis must equal the first moment of the tensile area about the neutral axis. Therefore, taking the moment of top and bottom areas about the neutral axis, equating, and substituting the values of 'n' and 'A_{frp}' provides:

$350*(x)*(x/2) = nA_{frp}*(325–x)$. This quadratic equation in terms of neutral axis location is solved and yields: $x = 46.32$ mm.

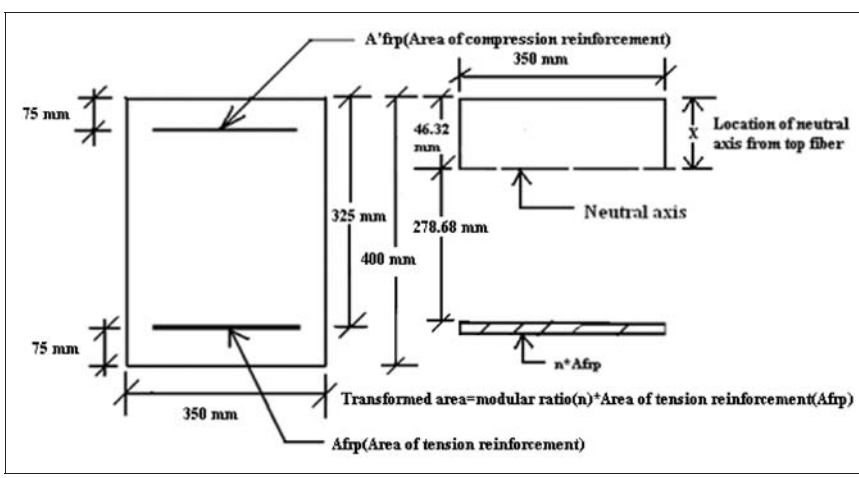

Figure 9. Beam cross-section and dimensions of transformed area.

Using this value of neutral axis location, the cracking moment of inertia about the neutral axis of the transformed section can now be calculated as: $1/3\,b(x)^3 + nA_{frp}(d–x)^2$, where b and d are respectively beam width, and the effective depth of beam cross-section (Figure 9). This provides: $I_{cr} = 1/3*(350)*(46.32)^3 + 1.35*1013.90*(325–46.32)^2 = 10.89 \times 10^7$ mm^4.

Similarly, the gross moment of inertia can be calculated from the beam cross-section in Figure 9 as: $I_g = 1/12\ bh^3$, where h is the height of the beam cross-section in Figure 9. This yields: $I_g = (1/12)*(350)*(400)^3 = 18.67 \times 10^8$ mm^4.

The cracking moment is the moment that, when exceeded, causes concrete to begin cracking. The cracking moment is found by setting the elastic flexural stress equation equal to the tensile stress capacity of the concrete, or, the value of $M_{cr} = (f_r\ I_g)/y_t$, where f_r is the modulus of rupture. This is the stress developed in the beam on the verge of tensile failure. By definition, $f_r = 0.7\ (f'_c)^{1/2}$ and $y_t = h/2$. This is the distance to the tensile edge from the neutral axis in the beam cross-section. Therefore, $f_r = 0.7(f'_c)^{1/2} = 0.7(41.8)^{1/2}$ N/mm^2 $= 4.53$ N/mm^2, and $M_{cr} = 4.53(18.67 \times 10^8)/200 = 4.2 \times 10^7$ N-mm.

The quantity, I_e, accounts for both the tension stiffening and the variation of moment of inertia along the beam. It is based on an estimation of the probable amount of cracking caused by the varying moment throughout the beam span. The value of I_e is always less than I_g. The equation used to calculate I_e is $I_e = (M_{cr}/M_a)^3\ I_g + [1–(M_{cr}/M_a)^3]I_{cr}$. Substitution of required parameters in this equation yields: $I_e = (4.2 \times 10^7/35.6 \times 10^7)^3 \times 18.67 \times 10^8 + \{1–(4.2 \times 10^7/35.6 \times 10^7)^3\} \times 10.89 \times 10^7 = 10.1 \times 10^7$ mm^4. This value is less than I_g, as expected.

Calculated and provided parameters can now be used to obtain the deflection constant and beam deflection. Therefore, $\psi = [2\ K_s*e*L*(A_{frp} + A'_{frp})]/I_{eff} = [2*0.49*125*4250*(1013.9 + 289.70)]/(10.1 \times 10^7) = 6.71$. Substitution of this into the deflection equation provides the deflection as: $\Delta_{et} = (\psi*\alpha_g*T_{frp}*E_{frp})/E_{conc} = (6.71*0.0465*435*3.6 \times 10^4)/30650 = 159.4$ mm. Therefore, % error $= (178.1–159.4)/178.1 \approx 10.3\%$.

Conclusions and future work

In this article, a new model is developed that incorporates the temperature-dependent progressive changes of E-modulus of FRP in predicting the deflection of FRP reinforced concrete structures within the range of practical elevated temperatures. Information presented has led to the following conclusions:

1. The model incorporates temperature-dependent progressive changes of E-modulus of FRP. The model is capable of predicting the deflection of FRP reinforced concrete structures within the range of practical elevated temperatures conservatively. This can provide an additional tool to evaluate the deflection of FRP reinforced concrete structures a in fire.

2. The predicted larger deflection values for beams 1 and 2 are approximately $L/28$ and $L/29$, respectively. These are lower than the maximum allowable limit of $L/20$ specified by BS 476.

Based on the mechanical property models for FRP materials proposed here, further work will be undertaken on flanged beams and slabs.

Funding

This research received no specific grant from any funding agency in the public, commercial, or not-for-profit sectors.

Nomenclature

A_g = area of glass
A_{frp} = tension reinforcement
A'_{frp} = compression reinforcement
A_m = area of matrix
b = width of beam
d = effective depth of the beam cross-section
e = distance from the tension reinforcement to neutral axis
E_{lt} = Young's modulus in the leathery zone
E_{conc} = Young's modulus of concrete
E_m = Young's modulus matrix
E_g = Young's modulus of glass
E_{frp} = Young's modulus of FRP rebar
f_r = modulus of rupture
f'_c = 28 days compressive strength of concrete
h = overall height of the beam cross-section
I_g = gross moment of inertia
I_{cr} = cracking moment of inertia
I_{eff} = effective moment of inertia
K_s = support conditions of the FRP system exposed to elevated temperatures
L = beam span
M_a = maximum applied moment
M_{cr} = cracking moment
M_r = reduction modulus
n_g = modular ratio up to leathery state
n_{lt} = modular ratio in the leathery zone
P_c = force in composite material
P_{frp} = force in FRP rebar
P_f = force in fiber
P_m = force in matrix
T_h = tension force due to shrinkage
V_g = volume of glass
V_m = volume of matrix
V_{lt} = volume in the leathery zone

x = location of neutral axis in the transformed area diagram
y_t = distance from neutral axis to extreme tension fiber
α_g = conversion of FRP at glassy state
α'_g = FRP expansion per degree variation of temperature
α_d = coefficient of expansion of FRP at decomposed state
T_{frp} = temperature at which deflection is evaluated
Δ_{et} = beam deflection at elevated temperature
Δ_{exp} = experimental deflection at elevated temperature
ε = Strain
ε_h = concrete strain due to elevated temperature
ξ = a conversion factor constant at particular temperature regime
ρ_f/ρ_b = ratio of GFRP to balanced GFRP
σ_{frp} = stress in FRP rebar
σ_g = stress in glass
σ_m = stress in matrix
Φ_{et} = shrinkage curvature due to elevated temperature
ψ = deflection constant

References

1. Nadjai A, Talamona D and Ali F. Fire performance of concrete beams reinforced with FRP bars. In: *Proceedings of the First International Symposium on Bond Behavior of FRP in Structures*. BBFS 2005, Hong Kong, 2005, pp.401–410.
2. ACI 440.1R-06. *Guide for the design and construction of structural concrete reinforced with FRP bars*. Farmington Hills, MI: American Concrete Institute, 2006, pp.1–45.
3. CSA, S806-02. *Design and construction of building components with fiber-reinforced polymer*. Mississauga, Canada: Canadian Standards Association, 2002.
4. ACI Committee 440. *Guide for the design and construction of externally bonded FRP systems for strengthening concrete structures*. ACI 440.2R-08. Farmington Hills, MI: American Concrete Institute, 2008, pp.1–45.
5. British Standards Institution. *Fire tests on building materials and structures part 21*: *Method of determination of fire resistance of elements of construction*. BS 476, United Kingdom: BSI, 1987.
6. British Standards Institution. *Code of practice for fire safety in the design, management and use of buildings*. BS 9999, United Kingdom: BSI, 2008.
7. Blontrock H, Taerwe L and Matthys S. Properties of fiber reinforced plastics at elevated temperatures with regard to fire resistance of reinforced concrete members. In: *Proceedings of 4th International Symposium on Non-Metallic (FRP) Reinforcement for Concrete Structures*, American Concrete Institute, Baltimore, MD, 1999, pp.43–45.
8. Bank LC. Properties of FRP reinforcements for concrete: fiber reinforced plastic (FRP) reinforcements for concrete structures. In: Nanni A (ed.) *Properties and applications*. London: Elsevier Science, 1993, pp.59–86.
9. Bakis CE. FRP reinforcement: material and manufacturing: fiber reinforced plastic (FRP) reinforcements for concrete structures. In: Nanni A (ed.) *Properties and Applications*. London: Elsevier Science, 1993, pp.13–58.

10. Wang YC, Wong PH and Kodur V. *Mechanical properties of fiber reinforced polymer reinforcing bars at elevated temperatures*. Canada: National Research Council Canada, 2003, NRCC-46121, pp.1–9.
11. Abbasi A and Hogg PJ. Fire testing of concrete beams with fibre reinforced plastic rebar. *Compos Part A: Appl Sci Manuf* 2006; Vol. 37(8): 1142–1150.
12. Ashby MF and Jones DRH. *Engineering materials: an introduction to microstructures, processing and design*. Oxford: Pergamon Press, 1999.
13. Bai Y, Keller T and Valle T. Modeling of stiffness of FRP composites under elevated and high temperatures. *Compos Sci Technol* 2008; Vol. 68: 3099–3106.
14. Saafi M. Effect of fire on FRP reinforced concrete members. *Compos Struct* 2008; Vol. 58: 11–20.
15. ACI 435R. *Control of deflection in concrete structures*. Farmington Hills, MI: American Concrete Institute, 1997, pp.1–77.